Natural Resources for Human Health

eISSN: 2583-1194

Original Research

Received : 02 Aug. 2026
Revised : 07 Sept. 2026
Accepted : 04 Oct. 2026
Publication : 12 Oct. 2026

Natural Resources for Human Health 2026, Vol. 6 (16s): 218–237

KEYWORDS:
Efinaconazole, Invasomes, Topical gel, Onychomycosis, Keratinized barrier, Antifungal, Drug permeation, Vesicular system.

Development and Optimization of Efinaconazole-Loaded Invasomal Gel for Enhanced Topical Delivery across Keratinized Biological Barriers and Antifungal Efficacy

Asifa Siddiqui[1], Kunal Arora[1*]

[1]Department of Pharmaceutics, Faculty of Pharmacy, Swami Vivekanand Subharti University, Meerut, Uttar Pradesh, India

*Corresponding author: Kunal Arora, Email: kunalarora.2009@rediffmail.com

ABSTRACT:

Background: The topical therapy of onychomycosis is problematic because of the highly keratinised nail barrier, impairing medication absorption and thereby reducing therapeutic effectiveness. Efinaconazole is a lipophilic triazole antifungal with low water solubility and limited penetration of keratinised tissues, limiting transungual delivery. The present study aimed to develop and optimize an efinaconazole-loaded invasomal gel to improve topical delivery across a keratinized biological barrier and enhance antifungal performance.

Methods: Invasomes loaded with efinaconazole were produced by thin film hydration process and optimised utilising DoE based methodology. The optimised formulation was included in a Carbopol gel and examined for vesicle features, physicochemical properties, in-vitro drug release, ex-vivo permeability, drug retention and in-vivo antifungal effectiveness in a Trichophyton rubrum-induced Wistar rat model.

Results: The optimised invasomal formulation showed vesicle size of 135 ± 3 nm, polydispersity index of 0.25 ± 0.01 and entrapment efficiency of 91.8 ± 0.7%. The invasomal gel exhibited appropriate pH, viscosity and spreadability for topical purposes. The optimized invasomal gel exhibited an initial rapid-release phase followed by a slower release phase, reaching 91.3 ± 2.5% cumulative release at 12 h and 94.6 ± 1.6% at 24 h.. Ex vivo permeation experiments using excised rat abdominal skin as a surrogate keratinized membrane showed substantially greater drug permeation and skin retention from the optimized invasomal gel than from the conventional gel.

Conclusion: The optimized invasomal gel demonstrated improved physicochemical characteristics, drug permeation, skin retention, and antifungal activity. However, permeation was evaluated using excised rat skin as a surrogate keratinized membrane; therefore, further studies using validated nail permeation models are warranted.

1. INTRODUCTION

Onychomycosis is a common fungal nail infection characterized by nail discoloration, thickening, and deformity. The dense, keratinized nail plate presents a major barrier to topical drug penetration, resulting in inadequate drug exposure and prolonged treatment [1–3].

Efinaconazole is a triazole antifungal that inhibits ergosterol synthesis. However, its physicochemical properties can limit topical delivery and penetration through keratinized tissues [4,5]. Invasomes, composed of phospholipids, ethanol, and terpenes, offer a promising vesicular approach for enhancing drug permeation through biological barriers [6,7]. Although efinaconazole has been investigated in other nanovesicular systems [8], invasomal gel-based delivery remains insufficiently explored.

Therefore, the present study aimed to develop and optimize an efinaconazole-loaded invasomal gel using a Design of Experiments (DoE) approach and evaluate its vesicular characteristics, drug release, permeation, retention, and in-vivo antifungal activity. Ex-vivo permeation was assessed using rat skin as a surrogate keratinized membrane; therefore, these findings do not represent direct transungual permeation.

2. MATERIALS AND METHODS

2.1 Materials

Efinaconazole (>99% purity) was **received as a gift sample from Sun Pharmaceutical Industries Ltd. (Mumbai, India)**. Soya phosphatidylcholine (SPC; Lipoid S100; ≥95% phosphatidylcholine) was obtained from Lipoid GmbH (Germany) through Lipoid India Pvt. Ltd. (Mumbai, India). Analytical-grade ethanol (≥99.5%) and triethanolamine were obtained from Merck Life Science Pvt. Ltd. (Mumbai, India). Limonene (≥97% purity), a terpene-based permeation enhancer, was purchased from Sigma-Aldrich India Pvt. Ltd. (Bengaluru, India) [11] [12] [13].

Carbopol 934 NF grade was obtained from Colorcon Asia Pvt. Ltd. (Goa, India). Propylene glycol (analytical grade), used as a cosolvent and humectant, was obtained from Rankem (Avantor Performance Materials India Ltd., Gurugram, India). **All chemicals and reagents were used as received without further purification unless otherwise stated. Double-distilled water was used throughout the study** [14] [15].

2.2 Preformulation Studies

Preformulation studies were conducted to characterize efinaconazole and establish suitable analytical conditions for formulation development and evaluation [16].

2.2.1 Physical Appearance

The colour, odour, and physical appearance of efinaconazole were examined visually to assess its general organoleptic characteristics [17].

2.2.2 Melting Point Examination

The melting point of efinaconazole was determined by the open-capillary method using a digital melting point apparatus. The observed melting range was compared with reported literature values to support drug identity and purity [18] [19].

2.2.3 Determination of λmax

An efinaconazole standard solution (10 μg/mL) was prepared in a suitable solvent and scanned from 200 to 400 nm using a UV–Visible spectrophotometer (Shimadzu UV-1800, Japan). The wavelength of maximum absorbance (λmax) was identified as 210 nm and used for subsequent quantitative analysis and calibration-curve preparation [20].

2.2.4 Solubility Study

The solubility of efinaconazole was evaluated by the shake-flask method in distilled water, 0.1 N HCl, 0.1 N NaOH, methanol, ethanol, chloroform, and phosphate buffer (pH 6.8). An excess amount of drug was added to each solvent and equilibrated under continuous stirring for 24 h at room temperature. The solutions were filtered and analyzed spectrophotometrically at 210 nm.

2.2.5 Calibration Curve

A stock solution of efinaconazole was serially diluted to prepare standard solutions over the required concentration range. Absorbance was measured at 210 nm using a UV–Visible spectrophotometer. A calibration curve of absorbance versus concentration was constructed, and the regression equation and correlation coefficient (R^2) were determined.

2.3 Structure of Pseudo-Ternary Phase Diagram

A pseudo-ternary phase diagram was constructed using the water-titration method to identify the composition range capable of forming visually stable invasomal dispersions . SPC and limonene constituted the lipid/terpene phase, ethanol served as the cosolvent and penetration enhancer, and distilled water constituted the aqueous phase. SPC and limonene were mixed at predetermined ratios, followed by gradual addition of ethanol (20–40% v/v). Distilled water was then added dropwise under continuous stirring at room temperature until a visible change in clarity or phase behavior occurred. The resulting systems were

visually evaluated for clarity, turbidity, and phase separation. Compositions showing clear or slightly translucent appearance without visible phase separation were identified as the vesicle-forming region and used to define the composition range for the subsequent 3^2 factorial design.

2.4 Preparation of Invasomes

Efinaconazole-loaded invasomes were prepared by a modified thin-film hydration method [30–32]. Efinaconazole and soy phosphatidylcholine (SPC) were dissolved in chloroform:methanol (2:1, v/v), followed by solvent evaporation at 40 °C under reduced pressure to form a thin lipid film. The film was vacuum-dried for 2–3 h and hydrated with ethanol–limonene aqueous phase (limonene 1% v/v) at 40 ± 2 °C for 30–60 min. The dispersion was probe-sonicated for 5–10 min and stored at 4 ± 1 °C .

A 3^2 full factorial design was used to study SPC (X_1: 1–3% w/v) and ethanol (X_2: 20–40% v/v), while limonene was fixed at 1% v/v. Nine formulations (F1–F9) were evaluated for vesicle size, entrapment efficiency, and PDI.

2.5 Optimization Strategy

A 3^2 full factorial DoE was used to evaluate the effects of SPC concentration (X_1, 1–3% w/v) and ethanol concentration (X_2, 20–40% v/v), while limonene was fixed at 1% v/v. Vesicle size (Y_1), entrapment efficiency (Y_2), and PDI (Y_3) were selected as responses. Nine formulations (F1–F9) were prepared and analyzed using Design-Expert software. ANOVA was used to assess model significance and adequacy, and response-surface/contour plots were generated. Numerical optimization was performed using desirability to minimize vesicle size and PDI while maximizing entrapment efficiency.

2.6 Characterization of Invasomes

The optimized invasomal formulation was characterized for vesicle size, PDI, zeta potential, entrapment efficiency, and morphology to assess its physicochemical characteristics and vesicular uniformity .

2.6.1 Particle Size and Polydispersity Index (PDI)

Vesicle size and PDI were measured by dynamic light scattering using a Malvern Zetasizer Nano ZS at 25 ± 1 °C after suitable dilution with double-distilled water. Z-average diameter and PDI were recorded, with PDI <0.30 indicating a relatively homogeneous distribution.

2.6.2 Zeta Potential

The zeta potential of the invasomal vesicles was determined from electrophoretic mobility using the same instrument with a folded capillary cell at 25 ± 1 °C. Zeta potential was used to assess the surface charge and electrostatic contribution to colloidal stability. Greater absolute zeta-potential values generally indicate stronger electrostatic repulsion and reduced aggregation [45] [46].

2.6.3 Entrapment Efficiency (EE %)

Invasomal dispersion was centrifuged at 15,000 rpm for 30 min at 4 °C, and unentrapped efinaconazole in the supernatant was quantified spectrophotometrically at 210 nm. EE% was calculated as the percentage of drug entrapped within the vesicles [47].

$$EE(\%) = \frac{\text{Total Drug} - \text{Free Drug}}{\text{Total Drug}} \times 100$$

Higher entrapment efficiency indicates greater incorporation of efinaconazole within the vesicular system.

2.6.4 Morphological Analysis

The morphology of the optimized invasomal vesicles was examined by scanning electron microscopy (SEM). The sample was appropriately prepared, mounted on an aluminum stub, and coated with a thin layer of gold under vacuum before imaging (Zeiss, Germany). The resulting micrographs were evaluated for vesicle shape, surface morphology, and aggregation.

2.7 Preparation of Invasomal Gel

The optimized invasomal dispersion (F6) was incorporated into a Carbopol 934 gel base to improve topical applicability and residence time at the site of application. Carbopol 934 (1% w/w) was selected as the gelling agent because of its suitable rheological and bioadhesive properties.

Carbopol 934 was accurately weighed, dispersed in double-distilled water, and allowed to hydrate at room temperature for 4–6 h with gentle stirring to obtain a uniform gel base. The optimized efinaconazole-loaded invasomal dispersion was gradually incorporated into the hydrated Carbopol base with continuous gentle mixing to minimize disruption of the vesicles. Propylene glycol (10% w/w) was incorporated as a cosolvent and humectant. Triethanolamine was added gradually to adjust the formulation to pH 5.5–6.5 and obtain the desired gel consistency. The final formulation was gently homogenized to ensure uniformity and minimize air entrapment and was stored at 4 ± 1 °C until further evaluation.

2.8 Evaluation of Invasomal Gel

The optimized invasomal gel was evaluated for appearance, homogeneity, pH, viscosity, spreadability, drug content, and extrudability. All parameters were assessed using standard methods in triplicate (n = 3) and expressed as mean ± SD.

2.9 In Vitro Drug Release Study

Drug release from optimized invasomal gel was evaluated using a Franz diffusion cell with dialysis membrane. Phosphate buffer (pH 5.5) containing 20% v/v ethanol was used as receptor medium at 37 ± 0.5 °C. Gel (100 mg; 1 mg efinaconazole) was applied, and samples were collected up to 24 h and analyzed at 210 nm. Release data were fitted to kinetic models. The study was performed in triplicate.

2.10 Ex Vivo Permeation Study

Ex vivo permeation through excised rat abdominal skin was studied using a Franz diffusion cell. Phosphate buffer (pH 5.5) containing 20% v/v ethanol was maintained at 37 ± 0.5 °C. Optimized gel (100 mg; 1 mg efinaconazole) was applied over 1.76 cm^2 skin area. Cumulative permeation, flux, permeability coefficient (Kp), and enhancement ratio (ER) were determined (n = 3).

2.12 In Vivo Antifungal Study

The antifungal efficacy of optimized invasomal gel was evaluated in Wistar rats following IAEC approval (05.08.2024) and CPCSEA guidelines. Onychomycosis was induced using standardized T. rubrum inoculation, and treatment was initiated after infection establishment. Animals were divided into normal control, disease control, marketed formulation, and optimized gel groups (n = 6) and treated once daily for 21 days. Efficacy was assessed using nail thickness, discoloration, fungal burden (log CFU/nail), and local tolerability.

2.13 Stability Studies

Optimized invasomal gel was stored for 3 months at 4 ± 2 °C, 25 ± 2 °C/60 ± 5% RH, and 40 ± 2 °C/75 ± 5% RH according to ICH Q1A(R2). Samples were evaluated for appearance, pH, viscosity, drug content, and entrapment efficiency at predetermined intervals. Results were expressed as mean ± SD, and degradation rate and t90 were calculated.

3. RESULT AND DISCUSSION

3.1 Preformulation Study

Preformulation studies confirmed the suitability of efinaconazole for formulation development. The drug appeared as a white-to-off-white crystalline powder with a melting point of 124–126 °C, consistent with reported values. UV analysis showed λmax at 210 nm with good linearity over 2–10 μg/mL (R^2 = 0.9992). Efinaconazole exhibited poor aqueous solubility but higher solubility in methanol and ethanol. Its higher ethanol solubility supports incorporation into the ethanol-containing invasomal system, while the phospholipid–ethanol–limonene combination provides a rational approach for enhancing drug solubilization, permeation, and retention.

Table 5: Solubility of Efinaconazole in Selected Excipients used for Invasomal Formulation

S. No.	Excipient	Solubility (mg/mL)
1	Phospholipid (Soya lecithin)	52.3
2	Cholesterol	15.8
3	Ethanol	92.4
4	Transcutol® P	68.7
5	Propylene Glycol	45.6
6	Span 80	12.6
7	Tween 80	18.9
8	Carbopol 934	4.3
9	HPMC K4M	6.2

Note: Values are expressed as mean ± SD (n = 3). Ethanol showed the highest efinaconazole solubility (92.4 mg/mL), followed by Transcutol® P (68.7 mg/mL) and soya lecithin (52.3 mg/mL), supporting their selection as formulation components. Propylene glycol and Carbopol 934 showed lower solubilization but were retained as cosolvent/humectant and gelling agent, respectively.

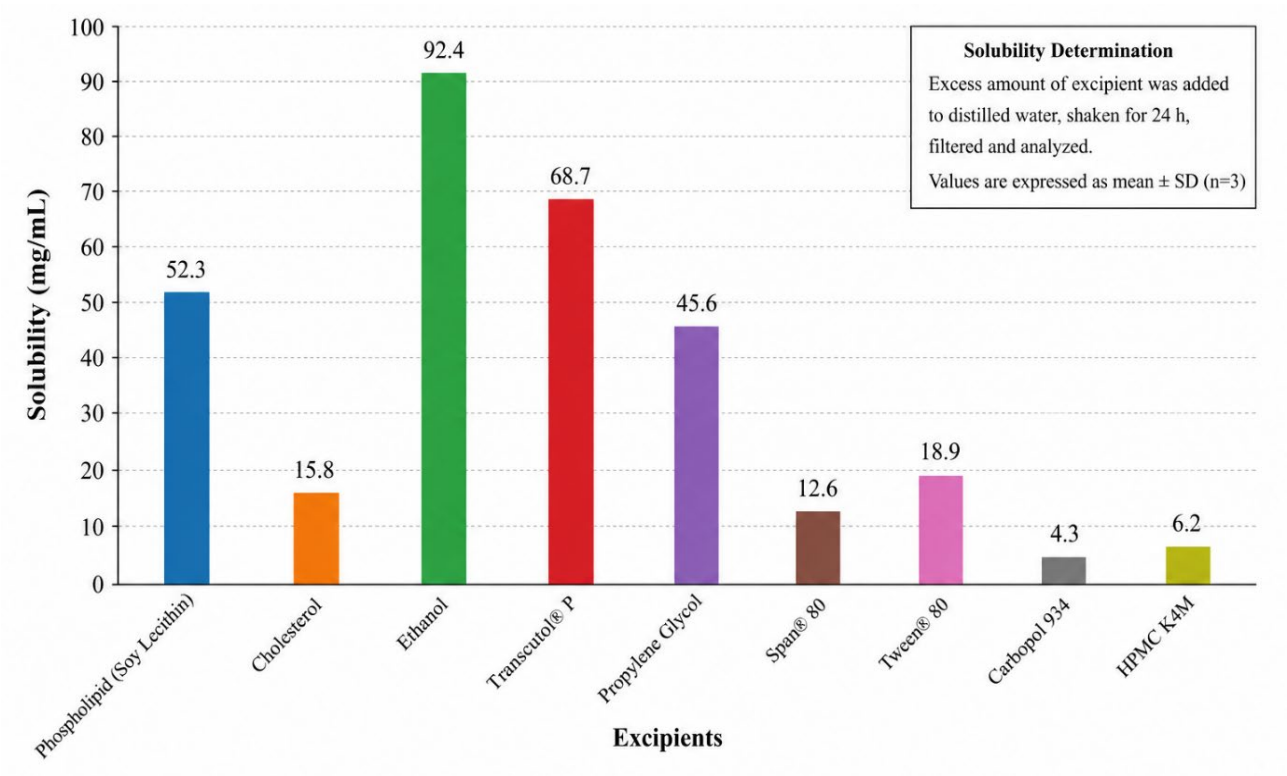

Figure 1: Solubility profile of efinaconazole in selected solvents and excipients.

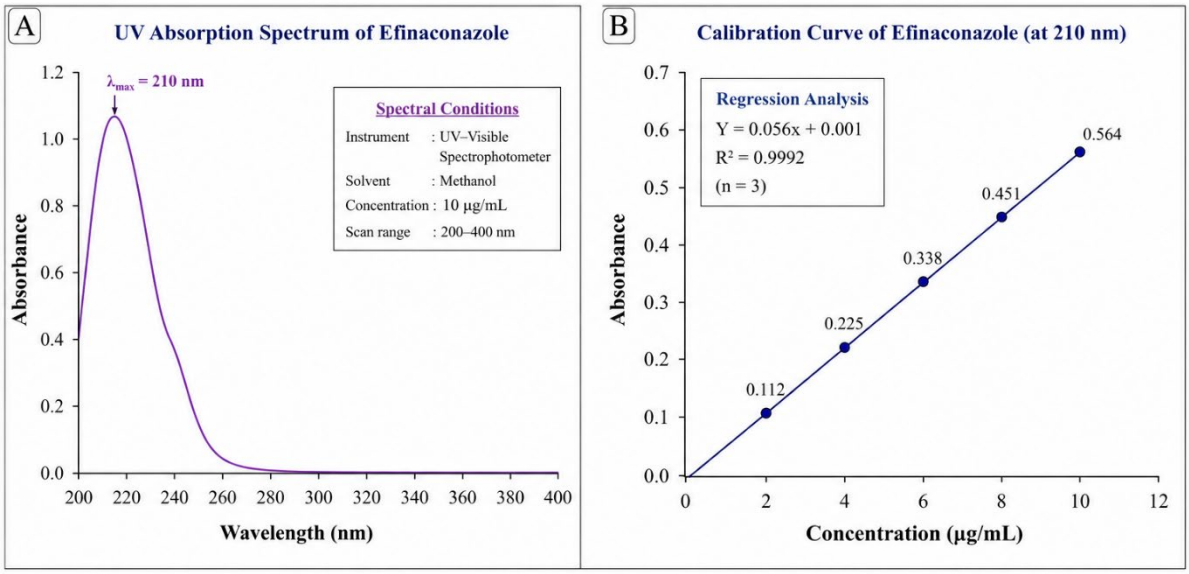

Figure 2. UV spectrum and calibration curve of efinaconazole showing λmax at 210 nm and linearity over the concentration range of 2–10 µg/mL (R^2 = 0.9992).

3.2 Pseudo-Ternary Phase Behavior and Vesicle Formation Region

The pseudo-ternary phase diagram identified a clear vesicle-forming region at moderate phospholipid (1–3% w/v) and high ethanol (30–40% v/v) concentrations. Low-ethanol or high-aqueous systems were turbid and unstable, indicating poor vesicle formation. Higher ethanol levels likely enhanced phospholipid fluidization, membrane flexibility, and vesicle deformability. At 1% v/v, limonene maintained vesicle integrity while promoting membrane flexibility and drug permeation through its lipophilic nature.

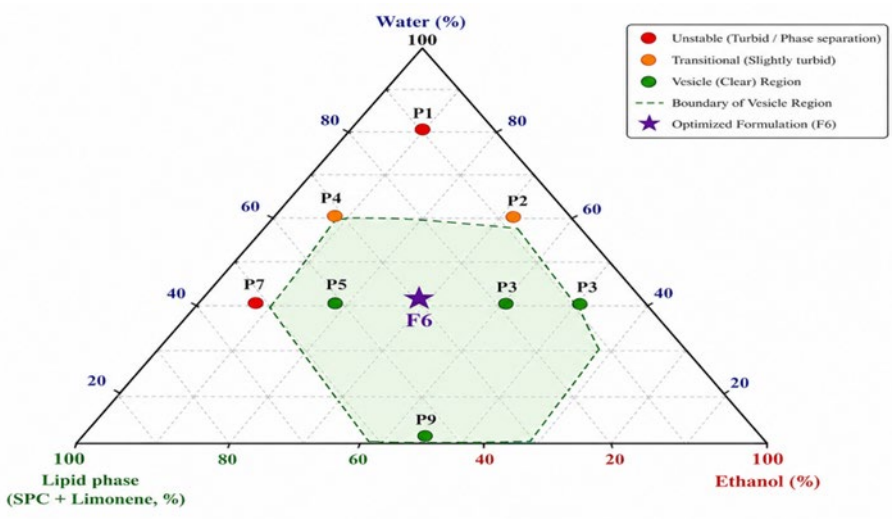

Figure 3. Pseudo-ternary phase diagram showing the vesicle-forming region; F1–F9 were selected within or near this region, with F6 (2% phospholipid, 40% ethanol) showing desirable vesicle formation for DoE optimization.

3.3 Optimization Results and Effect of Formulation Variables

A 3^2 factorial design evaluated the effects of phospholipid and ethanol concentrations on vesicle size, EE, and PDI (Table 6). Vesicle size ranged from 135 ± 3 to 210 ± 6 nm, with higher phospholipid levels increasing size, while ethanol reduced it through bilayer fluidization. EE ranged from 85.2 ± 1.2% to 91.8 ± 0.7%, generally increasing with phospholipid concentration but slightly decreasing at higher ethanol levels. Overall, phospholipid predominantly affected vesicle size and EE, whereas

ethanol influenced size and PDI. F6 (2% phospholipid, 40% ethanol) showed the smallest vesicles, highest EE, and lowest PDI, making it the most desirable formulation.

Table 6. Experimental design and observed responses of invasomal formulations (F1–F9).

Formulation	Lipid (% w/v)	Ethanol (% v/v)	Vesicle Size (nm)	EE (%)	PDI	Desirability
F1	1.0	20	210 ± 6	85.2 ± 1.2	0.34 ± 0.02	0.45
F2	1.0	30	185 ± 5	87.8 ± 1.0	0.31 ± 0.01	0.60
F3	1.0	40	160 ± 4	89.5 ± 0.9	0.29 ± 0.02	0.72
F4	2.0	20	175 ± 5	90.2 ± 1.1	0.30 ± 0.01	0.75
F5	2.0	30	150 ± 4	91.0 ± 0.8	0.27 ± 0.02	0.88
F6	**2.0**	**40**	**135 ± 3**	**91.8 ± 0.7**	**0.25 ± 0.01**	**0.98**
F7	3.0	20	145 ± 4	90.5 ± 0.9	0.28 ± 0.02	0.80
F8	3.0	30	165 ± 5	88.9 ± 1.0	0.30 ± 0.02	0.65
F9	3.0	40	155 ± 4	89.7 ± 0.8	0.29 ± 0.01	0.70

Note: Values are articulated as mean ± SD (n = 3).

3.3.1 Statistical Analysis and Model Fitting

ANOVA was performed to evaluate the statistical significance of the fitted models and the effects of phospholipid concentration (A) and ethanol concentration (B) on vesicle size (Y_1), entrapment efficiency (Y_2), and PDI (Y_3). Because both formulation variables were quantitative and investigated at three levels, the response models were evaluated using appropriate linear, interaction, and quadratic terms. Model adequacy was assessed using the coefficient of determination (R^2), adjusted R^2, predicted R^2, and lack-of-fit analysis.

For vesicle size (Y_1), phospholipid concentration showed a significant effect, while ethanol concentration also significantly affected vesicle size. The observed reduction in vesicle size with increasing ethanol concentration is consistent with ethanol-mediated membrane fluidization and increased vesicle deformability.

For entrapment efficiency (Y_2), phospholipid concentration showed a significant positive effect, consistent with increased availability of phospholipid bilayer domains for incorporation of the lipophilic drug. The effect of ethanol was concentration-dependent, with higher ethanol levels showing a tendency toward reduced drug retention, which may be related to increased membrane permeability and drug leakage.

For PDI (Y_3), ethanol concentration contributed significantly to the observed reduction in PDI, indicating improved vesicle-size uniformity within the investigated formulation range. The combined effects of the formulation variables demonstrate that optimization required simultaneous consideration of vesicle size, EE, and PDI rather than optimization of any single response. The significant model terms and the resulting response-surface analysis provided the basis for numerical optimization of the formulation.

Table 7: ANOVA for Vesicle Size (Y_1)

Source	SS	df	MS	F-value	p-value
Model	8425.36	5	1685.07	32.45	<0.0001
A	5120.22	1	5120.22	98.60	<0.0001
B	2310.45	1	2310.45	44.50	<0.0001
C	412.67	1	412.67	7.95	0.018

AB	315.12	1	315.12	6.08	0.032
Residual	311.50	6	51.92	—	—

R^2 = 0.982, Adjusted R^2 = 0.965, anticipated R^2 = 0.948, Lack of fit: non-significant

Table 8: ANOVA for Entrapment Efficiency (Y_2)

Source	SS	df	MS	F-value	p-value
Model	128.42	5	25.68	29.12	<0.0001
A	74.55	1	74.55	84.60	<0.0001
B	22.14	1	22.14	25.10	0.001
C	11.30	1	11.30	12.80	0.008
AB	8.65	1	8.65	9.80	0.014
Residual	5.29	6	0.88	—	—

R^2 = 0.975, Adjusted R^2 = 0.958, anticipated R^2 = 0.940, Lack of fit: non-significant

Table 9: ANOVA for Polydispersity Index (Y_3)

Source	SS	df	MS	F-value	p-value
Model	0.0124	5	0.00248	21.35	<0.0001
A	0.0058	1	0.0058	49.90	<0.0001
B	0.0036	1	0.0036	31.00	<0.0001
C	0.0012	1	0.0012	10.30	0.012
Residual	0.0007	6	0.00012	—	—

R^2 = 0.968, Adjusted R^2 = 0.950, anticipated R^2 = 0.932, Lack of fit: non-significant

The polynomial equations further confirmed that lipid concentration had an optimistic result, whereas ethanol showed a harmful outcome on vesicle size.

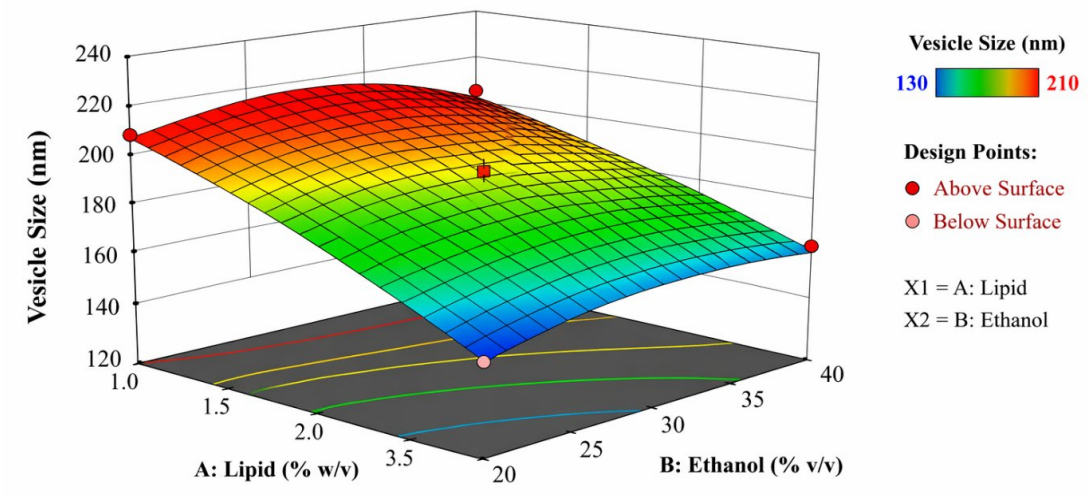

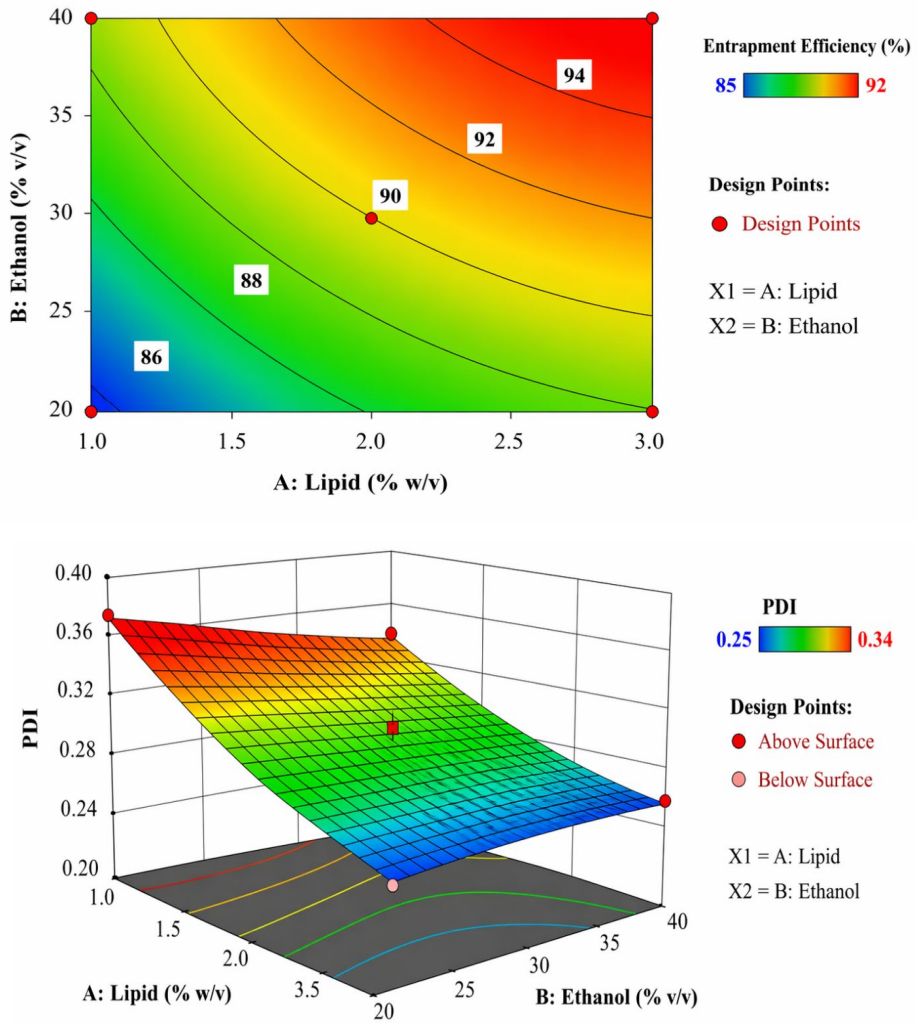

Figure 4: Depicts a response surface and a contour plot that describe the influence of phospholipid (A) and ethanol (B) concentrations on the size (Y_1), entrapment efficiency (Y_2), and polydispersity index (Y_3) of efinaconazole-loaded invasomes. The greater concentration of phospholipids, the larger the size of the vesicles and the entrapment rate. Fluidization of the membrane decreased the size of vesicles and PDI with escalating ethanol concentration. This enhanced the uniformity of vesicles

3.3.2 Optimization and Validation of Formulation

The optimal formulation was selected using a numerical desirability function with the objectives of minimizing vesicle size and PDI while maximizing entrapment efficiency. Among all formulations, F6 showed the most desirable combination of responses, with a vesicle size of 135 ± 3 nm, EE of 91.8 ± 0.7%, and PDI of 0.25 ± 0.01. The nanosized vesicles and relatively low PDI indicate a homogeneous vesicular population and may favor increased interfacial contact with keratinized tissues, thereby supporting improved drug deposition and permeation. The high desirability value (0.98) indicated that F6 provided the most favorable simultaneous optimization of the predefined formulation responses within the investigated design space.

The optimized formulation was subsequently prepared independently and evaluated to validate the predictive performance of the fitted models. The experimental values showed close agreement with the predicted values, with percentage deviations below 5% for all responses. The predicted vesicle size was 130.5 nm compared with the experimental value of 135 ± 3 nm, while the predicted EE and PDI were 90.9% and 0.24, respectively, compared with experimental values of 91.8 ± 0.7% and 0.25 ± 0.01%. The low prediction errors support the suitability of the DoE-based optimization for identifying formulation conditions that produce the targeted vesicular characteristics.

Table 10: Validation of Optimized Formulation (F6)

Response	Predicted Value	Experimental Value	% Error
Vesicle Size (nm)	**130.5**	**135 ± 3**	**3.45**
Entrapment Efficiency (%)	**90.9**	**91.8 ± 0.7**	**0.99**
Polydispersity Index (PDI)	**0.24**	**0.25 ± 0.01**	**4.17**

Note: Values are expressed as mean ± SD (n = 3). Percentage error was calculated relative to predicted values.

3.4 Vesicle description

Vesicle size, polydispersity index (PDI), and zeta potential of the optimized invasomal formulation (F6) were evaluated to assess its physicochemical characteristics and colloidal properties. Table 11 summarizes the results. The optimized preparation showed a vesicle size of 135 ± 3 nm, confirming the formation of nanosized vesicles. The small vesicle size provides a relatively high surface area and may facilitate close interaction with biological barriers, potentially supporting improved topical drug deposition and permeation. The PDI value of 0.25 ± 0.01 indicated a relatively narrow and homogeneous vesicle size distribution. The low PDI indicates good size uniformity and suggests a reduced tendency toward vesicle aggregation within the formulation.

The zeta potential of the optimized preparation was −21.6 ± 1.4 mV, indicating moderate surface charge and contributing to colloidal stability. Although the zeta potential value was below the conventional ±30 mV criterion commonly associated with electrostatic stabilization, the observed colloidal characteristics may also be influenced by non-electrostatic stabilization mechanisms associated with the formulation components. Ethanol can increase membrane fluidity and deformability, while the terpene component may influence interfacial and membrane interactions. Therefore, the measured zeta potential should be interpreted together with the particle-size distribution and physical appearance rather than as the sole indicator of formulation stability.

The particle size distribution profile (Figure 5) showed a relatively narrow distribution, further supporting vesicle uniformity. Similarly, the zeta potential distribution (Figure 6) indicated a predominantly negative surface charge consistent with the measured zeta potential.

Table 11 : Vesicle Characterization of Optimized Invasomal Formulation (F6)

Parameter	Value
Vesicle Size (nm)	135 ± 3
PDI	0.25 ± 0.01
Zeta Potential (mV)	−21.6 ± 1.4

Note: Values are indicated as mean ± SD (n = 3).

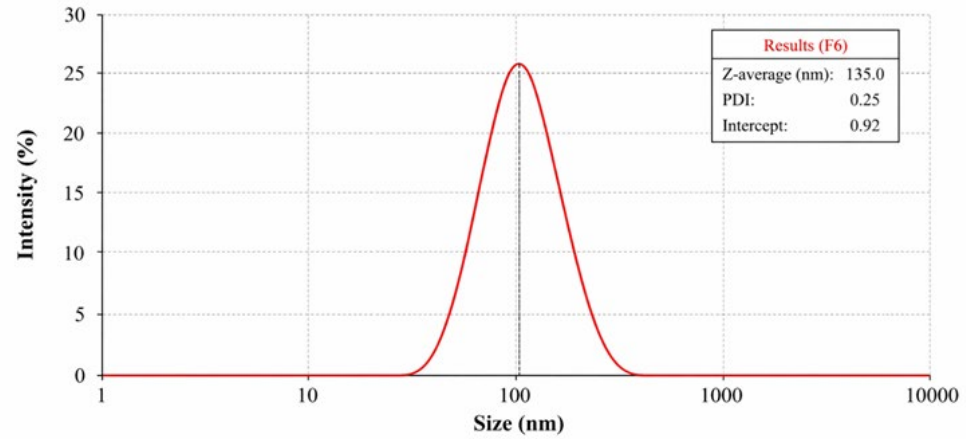

Figure 5: Particle Size Distribution of Optimized Invasomal Formulation (F6) Obtained by Dynamic Light Scattering

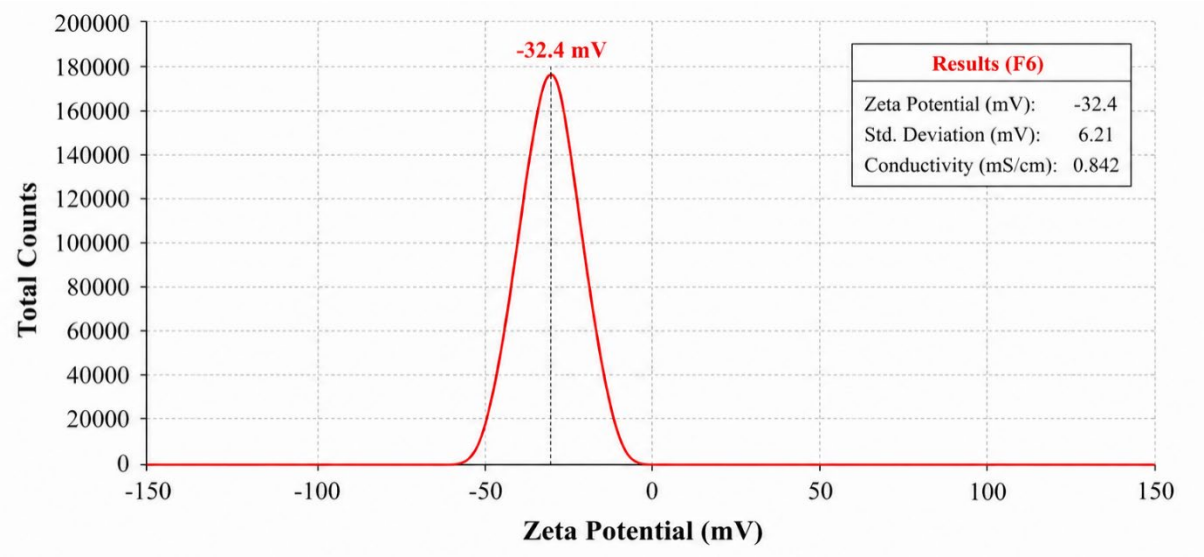

Figure 6 : Zeta-Potential Distribution of the Optimized Invasomal Formulation (F6), Showing a Predominantly Negative Surface Charge with a Measured Zeta Potential of −21.6 ± 1.4 mV.

3.5 Gel Evaluation

The optimized invasomal gel formulation (F6) was evaluated for its physicochemical characteristics, and the results are summarized in Table 12. The formulation showed no phase separation and appeared uniform, indicating homogeneous distribution of the vesicular system within the gel matrix.

The formulation's pH was within the physiologically acceptable range for skin (5.0–6.5), suggesting suitability for topical application. The absence of irritation observed during the subsequent in-vivo study further supported its local tolerability. The gel viscosity was 4820 ± 130 cP, indicating suitable consistency and retention characteristics for topical application. This viscosity may contribute to adequate residence at the application site while maintaining ease of application. The spreadability value (7.2 ± 0.4 g·cm/s) indicated good spreading properties, which are important for uniform drug distribution over the application site and patient compliance. The drug content (98.6 ± 0.7%) indicated uniform incorporation and distribution of efinaconazole within the gel matrix.

The rheological profile (Figure 8) showed that the gel exhibited pseudoplastic (shear-thinning) flow behavior, with a decrease in apparent viscosity with increasing shear rate. Such behavior is desirable for topical formulations because reduced viscosity under applied shear facilitates spreading during application, whereas higher viscosity under low-shear conditions may support retention at the application site. Likewise, the spreading profile (Figure 9) showed good spreading under applied stress, supporting convenient topical application and uniform distribution of the formulation. Overall, the optimized invasomal gel exhibited suitable pH, viscosity, spreadability, rheological behavior, and drug content for topical administration and subsequent performance evaluation.

Table 12. Physicochemical Evaluation of Optimized Invasomal Gel (F6)

Parameter	Value	Interpretation
Appearance	Smooth, homogeneous	No phase separation
pH	5.8 ± 0.2	Suitable for topical application
Viscosity (cP)	4820 ± 130	Suitable consistency
Spreadability (g·cm/s)	7.2 ± 0.4	Good spreading behavior
Drug Content (%)	98.6 ± 0.7	Uniform drug incorporation

Note: Values are indicated as mean ± SD (n = 3).

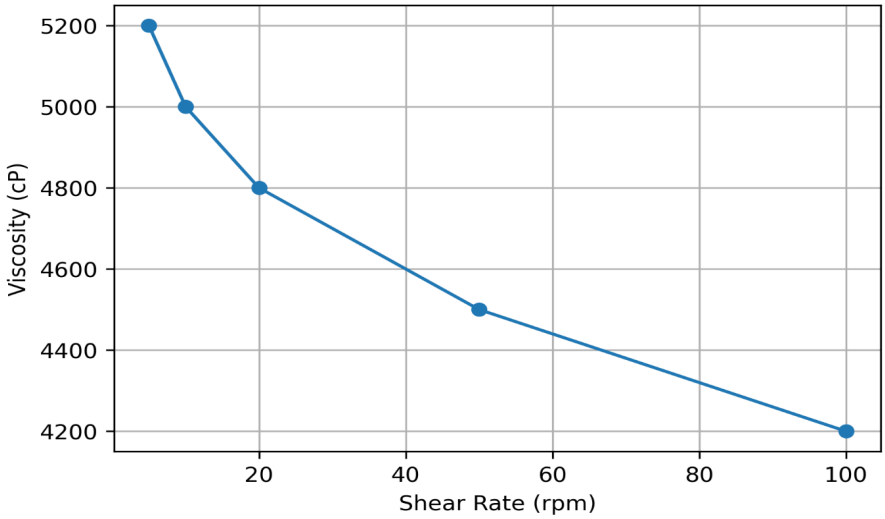

Figure 8: Rheological Profile of the Optimized Invasomal Gel (F6) Showing a Decrease in Apparent Viscosity with Increasing Shear Rate, Indicating Pseudoplastic (Shear-Thinning) Behavior Suitable for Topical Application

3.6 In-vitro Drug discharge

The in-vitro drug release profile of the optimized invasomal gel (F6) is reported in Tables 13 and 14 and Figure 9. The formulation showed an initial release of 18.5 ± 1.2% within 0.5 h, followed by progressive drug release to 91.3 ± 2.5% at 12 h and 94.6 ± 1.6% at 24 h. The release profile therefore demonstrated an initial relatively rapid-release phase followed by a slower release phase after 12 h.

Table 13: Cumulative Percentage Drug Release of Efinaconazole from Invasomal Formulations (F1–F9) at Different Time Intervals

Time (h)	F1	F2	F3	F4	F5	F6 (Optimized)	F7	F8	F9
0	0	0	0	0	0	0	0	0	0
1	12.3	14.1	16.5	18.2	19.8	26.8	15.6	17.2	18.9
2	18.7	21.4	24.8	27.3	29.5	38.6	23.2	25.6	27.8
4	28.5	31.6	35.2	38.7	41.3	55.2	33.8	36.4	39.2
6	36.9	40.5	44.8	48.9	52.6	68.4	42.3	45.1	48.7
8	44.2	48.6	52.9	57.3	61.5	79.6	50.7	53.6	57.1
10	50.8	55.4	60.2	64.8	69.3	85.4	57.9	61.2	65.4
12	56.3	61.7	66.8	71.5	76.2	91.3	63.4	67.1	70.9
24	68.5	74.2	79.6	84.8	88.9	94.6	75.3	80.5	83.7

Table 14 : Cumulative Percentage Drug Release from the Optimized Invasomal Gel (F6)

Time (h)	Cumulative Drug Release (%)
0.5	18.5 ± 1.2
1	26.8 ± 1.4
2	38.6 ± 1.6

4	55.2 ± 1.8
6	68.4 ± 2.0
8	79.6 ± 2.2
10	85.4 ± 2.3
12	91.3 ± 2.5
24	94.6 ± 1.6

Note: Values are indicated as mean ± SD (n = 3).

The initial release was attributed to readily accessible drug near the vesicle surface, followed by slower diffusion from the vesicular bilayer and Carbopol matrix. More than 90% of drug was released within 12 h, with only ~3.3% additional release up to 24 h, indicating an initial rapid phase followed by limited release rather than prolonged sustained release.

As shown in Figure 9, the optimized invasomal gel exhibited higher cumulative release than the marketed and plain gel formulations. This enhanced release may be attributed to ethanol and limonene, which improve membrane fluidity and vesicle deformability, facilitating drug diffusion.

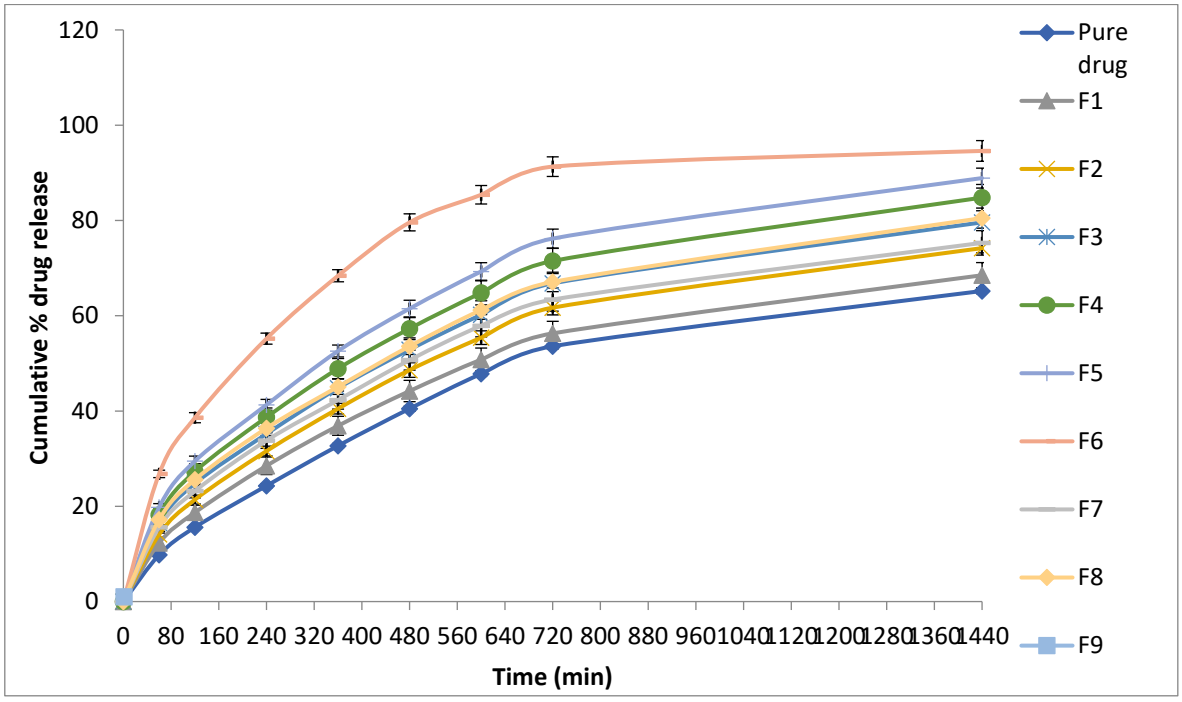

Figure 9: In-vitro cumulative drug release profile of efinaconazole from the optimized invasomal gel (F6), marketed formulation, and plain gel. The optimized invasomal gel exhibited a higher cumulative drug release, reaching 91.3 ± 2.5% at 12 h and 94.6 ± 1.6% at 24 h.

Table 16. Drug Release Kinetic Model Fitting

Model	Equation	R^2 Value
Zero-order	$Q = kt$	0.921
First-order	$\log Q = kt$	0.948
Higuchi	$Q = k\sqrt{t}$	0.982
Korsmeyer–Peppas	$M_t/M_\infty = kt^n$	**0.989**

The cumulative drug release data from the optimized invasomal gel (F6) were fitted to zero-order, first-order, Higuchi, and Korsmeyer–Peppas models (Table 16 and Figure 10). The Korsmeyer–Peppas model showed the highest correlation coefficient (R^2 = 0.989), followed by the Higuchi model (R^2 = 0.982), indicating that diffusion contributed substantially to the overall release process. The release exponent (n = 0.45–0.89) was consistent with anomalous/non-Fickian transport over the investigated range, suggesting contributions from both drug diffusion and relaxation of the polymeric/vesicular matrix. Thus, the release profile was governed predominantly by diffusion with a contribution from matrix relaxation rather than by simple zero-order release.

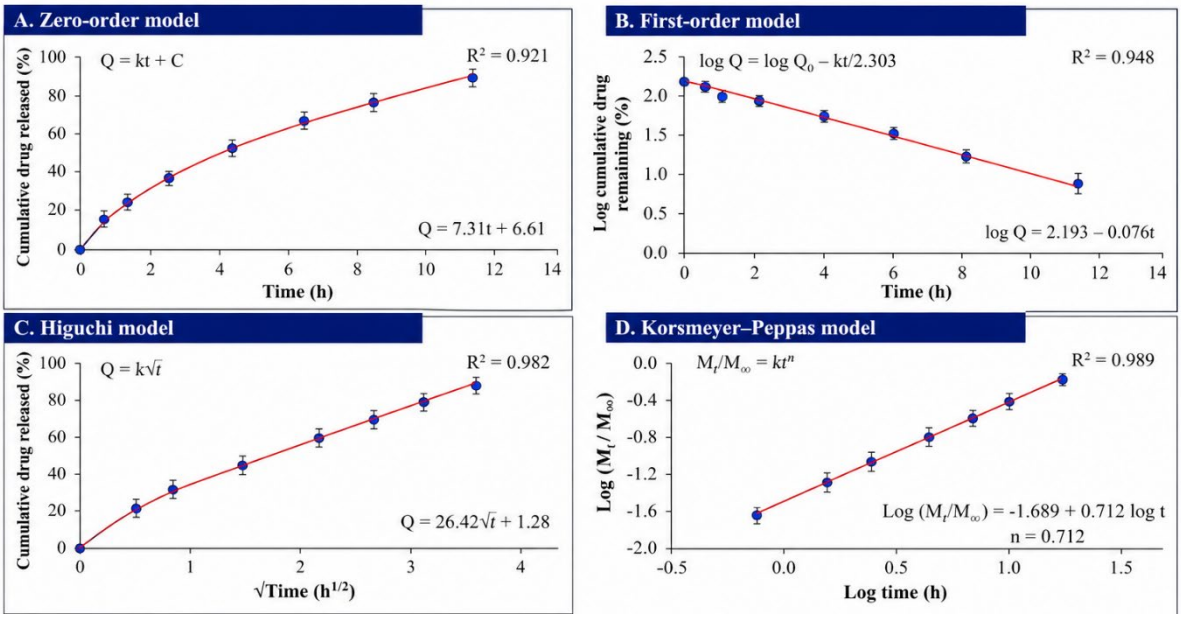

Figure 10: Drug-release kinetic model plots for the optimized invasomal gel (F6), showing the highest correlation with the Korsmeyer–Peppas model (R^2 = 0.989), followed by the Higuchi model (R^2 = 0.982).

3.7 Skin Permeation Study

As shown in Table 17 and Figure 11, the optimized invasomal gel (F6) showed significantly higher efinaconazole permeation than the conventional gel ($p < 0.05$), reaching 162.4 ± 3.2 μg/cm² at 12 h versus 95.7 ± 2.6 μg/cm², representing ~1.7-fold enhancement. The higher permeation and flux may be attributed to ethanol, limonene, and nanosized deformable vesicles (~135 nm), which enhance membrane interaction and drug diffusion. However, as rat skin was used as a surrogate membrane, these findings do not directly demonstrate transungual permeation.

Table 17. Ex Vivo Cumulative Drug Permeation Profile

Time (h)	Invasomal Gel (μg/cm²)	Conventional Gel (μg/cm²)
0.5	22.5 ± 1.3	10.2 ± 0.8
1	35.8 ± 1.5	16.4 ± 1.0
2	52.6 ± 1.8	24.7 ± 1.2
4	78.3 ± 2.1	38.5 ± 1.5
6	105.2 ± 2.5	54.6 ± 1.9
8	128.6 ± 2.8	69.3 ± 2.1
12	162.4 ± 3.2	95.7 ± 2.6

Note: Values are indicated as mean ± SD (n = 3).

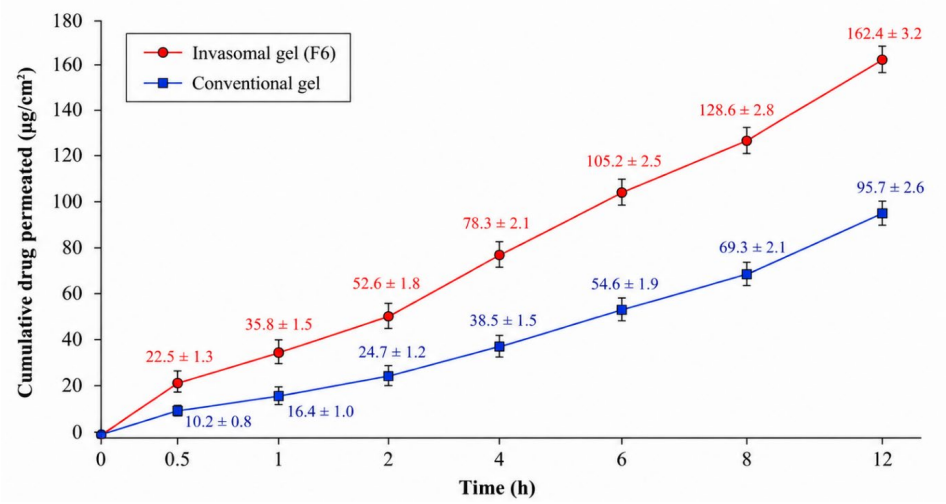

Figure 11. Cumulative ex-vivo permeation profile of efinaconazole from the optimized invasomal gel (F6) and conventional gel across excised rat skin. The invasomal gel showed higher cumulative permeation than the conventional gel, reaching 162.4 ± 3.2 µg/cm² at 12 h compared with 95.7 ± 2.6 µg/cm². Data are presented as mean ± SD (n = 3).

The permeation parameters are summarized in Table 18. The invasomal gel showed significantly higher steady-state flux (13.5 ± 0.6 µg/cm²/h) than the conventional gel (7.8 ± 0.4 µg/cm²/h) ($p < 0.05$). Similarly, the permeability coefficient (Kp) of the invasomal gel (0.0135 cm/h) was higher than that of the conventional gel (0.0078 cm/h). The enhancement ratio (ER) was 1.73, indicating an approximately 73% increase in steady-state flux relative to the conventional gel.

Table 18. Permeation Parameters

Parameter	Invasomal Gel (F6)	Conventional Gel
Flux (J, µg/cm²/h)	**13.5 ± 0.6**	7.8 ± 0.4
Permeability Coefficient (Kp, cm/h)	**0.0135** 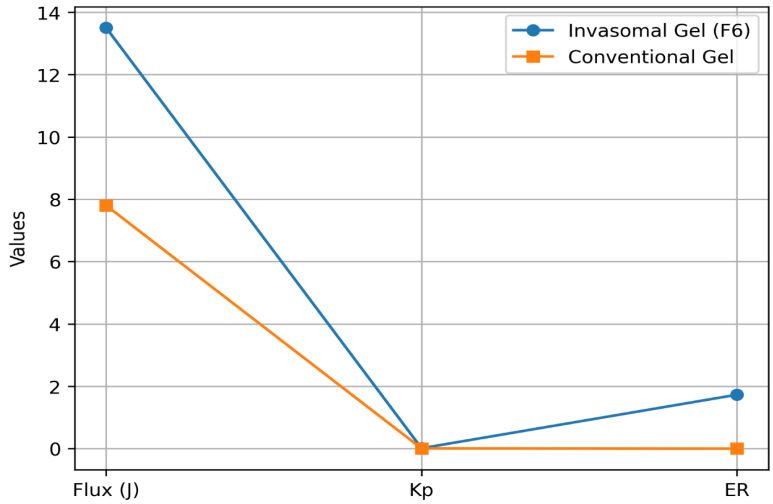	0.0078
Enhancement Ratio (ER)	**1.73**	—

Figure 12. Comparison of permeation parameters of efinaconazole from the optimized invasomal gel (F6) and conventional gel, including steady-state flux, permeability coefficient, and enhancement ratio.

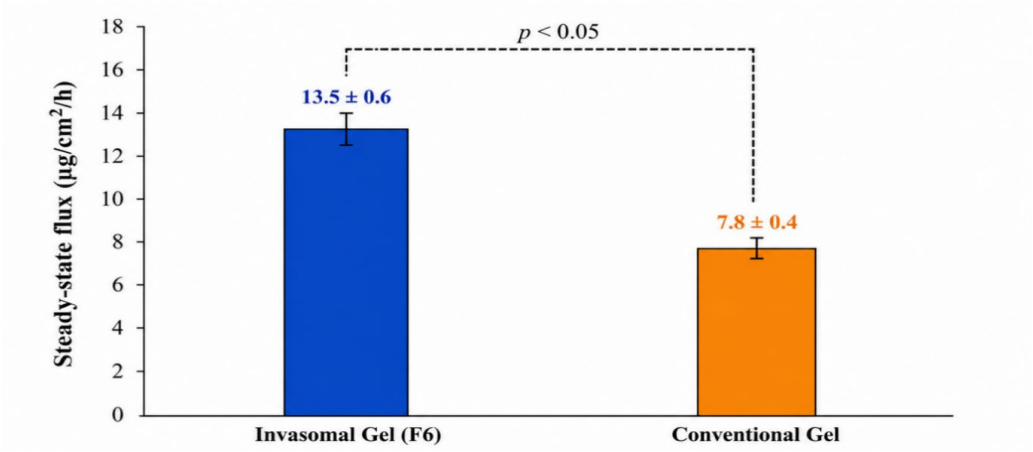

Figure 13. Steady-state permeation profile of efinaconazole across excised rat skin from the conventional and optimized invasomal gels (F6). The optimized invasomal gel exhibited a higher steady-state flux (13.5 ± 0.6 µg/cm²/h) than the conventional gel (7.8 ± 0.4 µg/cm²/h; $p < 0.05$). Data are presented as mean ± SD (n = 3).

The higher permeation parameters observed with the invasomal gel may be attributed to the combined effects of ethanol-mediated membrane fluidization, terpene-associated enhancement of drug partitioning, and the nanosized and deformable vesicular structure. These factors may facilitate closer interaction between the formulation and the membrane and thereby enhance drug transport. The enhanced ex-vivo permeation was consistent with the higher drug release observed for F6 in the in-vitro release study, suggesting that increased drug availability from the vesicular system contributed to the observed permeation enhancement. However, the present study used excised rat skin as a surrogate membrane; therefore, the results should not be interpreted as direct measurement of drug permeation through the human nail plate.

3.9 In Vivo Antifungal Study

The optimized invasomal gel (F6) was evaluated for antifungal activity in albino Wistar rats following establishment of the *Trichophyton rubrum*-induced infection. Four groups were evaluated: normal control, disease control, marketed formulation, and invasomal gel-treated group. Treatment was administered topically once daily for 21 consecutive days following confirmation of infection according to the predefined experimental criteria.

The disease control group exhibited progressive fungal infection, including increased nail thickness, marked discoloration, and elevated fungal burden. Conversely, animals treated with the invasomal gel showed improvement in the observed clinical parameters, including reduced nail thickness and improved nail appearance. Discoloration scores were also reduced compared with the disease-control group.

Microbiological evaluation showed that the invasomal gel reduced fungal burden to 2.20 ± 0.10 log CFU/nail, corresponding to approximately 53.7% reduction relative to the disease-control group, whereas the marketed formulation showed 2.35 ± 0.12 log CFU/nail, corresponding to approximately 50.5% reduction (Table 20). The difference between the invasomal gel and marketed formulation should be interpreted according to the statistical comparison performed between these two treatment groups. If this comparison was statistically significant ($p < 0.05$), the result may be described as a significant improvement; otherwise, the formulation should be described as showing a numerically greater reduction without claiming statistical superiority.

The improved antifungal response may be related to the enhanced drug permeation and skin retention observed in Sections 3.7 and 3.8. The nanosized and deformable vesicular system may facilitate closer interaction with keratinized tissue and increase local drug deposition, thereby contributing to the observed antifungal response. However, the present permeation and retention studies were performed using excised rat skin as a surrogate membrane and therefore do not directly establish enhanced drug delivery through the human nail plate.

During the treatment period, no erythema, edema, or other visible signs of irritation were observed, supporting the local tolerability of the formulation under the conditions of the study. Overall, the optimized invasomal gel demonstrated measurable antifungal activity and favorable topical tolerability in the experimental model.

Table 20. In Vivo Antifungal Evaluation

Parameter	Disease Control	Marketed	Invasomal Gel (F6)
Nail Thickness (mm)	1.85 ± 0.12	1.32 ± 0.10	**1.18 ± 0.08**
Discoloration Score (0–3)	3.0 ± 0.0	1.5 ± 0.3	**1.2 ± 0.2**
Fungal Burden (log CFU/nail)	4.75 ± 0.15	2.35 ± 0.12	**2.20 ± 0.10**
% Reduction in Fungal Burden	—	~50.5%	**~53.7%**
Irritation Score (0–4)	0	0	0

Note: Values are expressed as mean ± SD (n = 6). Statistical significance was evaluated using the predefined statistical test, with $p < 0.05$ considered significant. Pairwise comparisons between treatment groups should be reported where applicable.

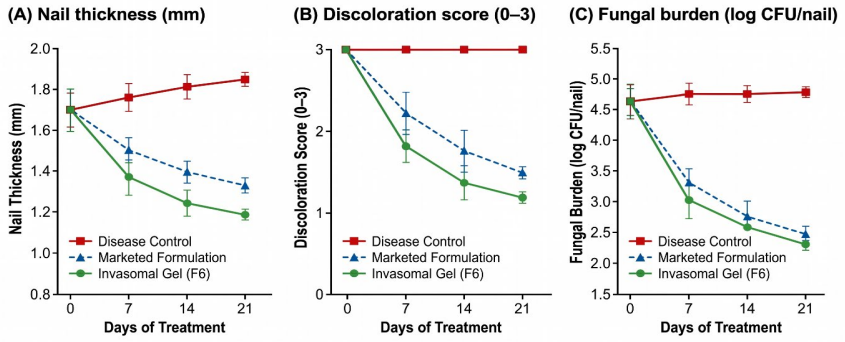

Figure 15. In-vivo antifungal efficacy of efinaconazole formulations in the T. rubrum-induced infection model: (A) nail thickness, (B) discoloration score, and (C) fungal burden. F6 improved clinical and microbiological parameters versus the disease-control group.

Figure 16. Representative images from the in-vivo *Trichophyton rubrum*-induced infection study in albino Wistar rats. (A) topical application of the test formulation to the infected site; (B) optimized invasomal formulation (F6); (C) representative treated nail showing improvement in appearance; (D) experimental animal housing/grouping; and (E) representative infected nail showing characteristic clinical changes.

3.10 Stability Study

The optimized invasomal gel (F6) was evaluated for physical and physicochemical stability over 3 months under refrigerated (4°C), room-temperature (25°C), and accelerated (40°C) storage conditions. The formulation remained physically stable, with no visible color change, phase separation, or drug crystallization during the study period. The pH remained within 6.4–6.8, with no statistically significant change under the investigated conditions ($p > 0.05$) . Viscosity showed a slight decrease over time, with a statistically significant change under accelerated storage at 40°C ($p < 0.05$), whereas the changes observed at 4°C and 25°C were not statistically significant.

Drug content remained above 95% throughout the study period; however, a significant decrease was observed under accelerated storage at 40°C ($p < 0.05$), whereas changes at 4°C and 25°C were not statistically significant. Entrapment efficiency also decreased gradually, with a significant reduction under accelerated storage at 40°C ($p < 0.05$), while changes under refrigerated and room-temperature conditions were not statistically significant. The greater changes observed at 40°C may be associated with increased membrane fluidity and greater molecular mobility, potentially promoting partial drug leakage from the vesicular system.

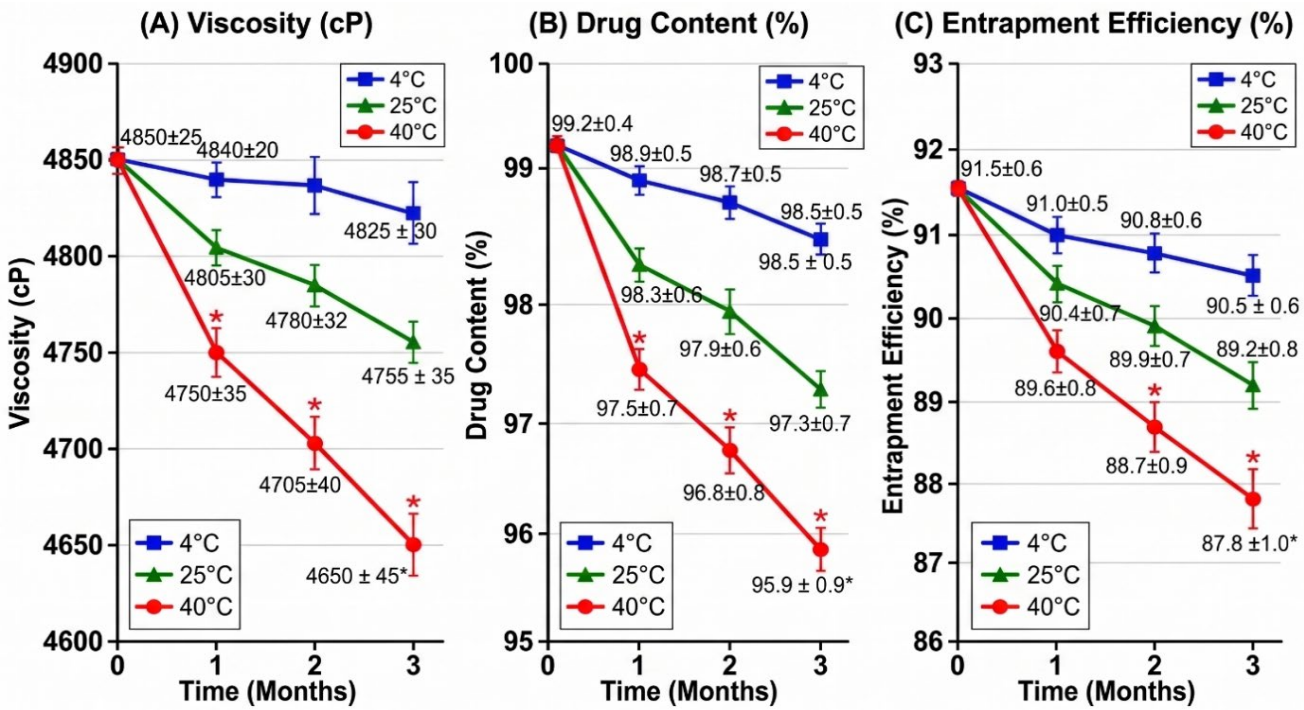

Figure 17: Stability profile of the optimized efinaconazole-loaded invasomal gel (F6) under refrigerated (4°C), room-temperature (25°C), and accelerated (40°C) storage conditions over 3 months. (A) drug content, (B) viscosity, and (C) entrapment efficiency. The formulation showed relatively limited changes at 4°C and 25°C, whereas greater changes were observed at 40°C, indicating temperature-dependent changes in formulation performance.

The optimized invasomal gel remained physically and physicochemically stable over 3 months under refrigerated and room-temperature conditions, while greater changes in viscosity, drug content, and entrapment efficiency were observed under accelerated storage at 40°C. The findings indicate temperature-dependent stability behavior, but longer-term real-time studies are required to establish the definitive shelf-life of the formulation

CONCLUSION

An efinaconazole-loaded invasomal gel was successfully designed and optimized using a Design of Experiments (DoE) approach to improve topical drug delivery. The optimized formulation exhibited nanosized vesicles, high entrapment efficiency, low polydispersity, and suitable physicochemical characteristics. Compared with the conventional gel, the optimized invasomal gel demonstrated enhanced efinaconazole permeation and skin retention in the ex-vivo rat-skin model, indicating improved drug transport and deposition.

REFERENCES

[1] J. J. Enriquez-Mendez and A. Gonzalez, "A Systematic Review on the Emerging Fungal Pathogen Neoscytalidium Causing Infections Worldwide," 2025. doi: 10.1007/s11046-025-00964-4.

[2] V. Saini, S. M. Safwan, D. Mehta, E. E. Das, and A. Bajaj, "Recent Advances in the Development of Antifungal Agents: Beyond Azoles, Polyenes, and Echinocandins," 2025. doi: 10.1021/acsinfecdis.4c00828.

[3] P. Ghasemiyeh, N. F. Haghighi, L. Dastgheib, S. Ranjbar, and S. Mohammadi-Samani, "Safety and efficacy of niosomal and conventional tranexamic acid/niacinamide vs. hydroquinone creams in melasma: A randomized, double-blind, case-controlled clinical trial," *Sci. Rep.*, 2025, doi: 10.1038/s41598-025-26693-8.

[4] A. K. Gupta, D. Taylor, D. Dennis, T. Wang, and E. A. Cooper, "Treating Onychomycosis with Efinaconazole: Considerations for Diverse Patient Groups," 2025. doi: 10.3390/jof11120843.

[5] S. W. Yun, J. G. Lee, C. H. Kim, and K. S. Kim, "Enhanced Efinaconazole Permeation and Activity Against Trichophyton rubrum and Trichophyton mentagrophytes with a Self-Nanoemulsifying Drug Delivery System," *Pharmaceutics*, 2025, doi: 10.3390/pharmaceutics17091230.

[6] C. Modi, B. G. Prajapati, D. U. Kapoor, and A. Mehta, "Transfersomes and Ethosomes for Psoriasis: A Review of Novel Vesicular Drug Delivery Systems," 2025. doi: 10.1007/s44174-025-00575-z.

[7] S. F. Elhabal, M. S. Farahat, M. H. Teaima, N. A. Elzohairy, and M. El-Nabarawi, "Innovate sodium alginate microneedle patches integrated with soft lidocaine invasomes: advanced strategies for oral ulcerative mucositis treatment via TNF-α/NF-κB pathways," *Drug Deliv. Transl. Res.*, 2025, doi: 10.1007/s13346-025-01915-8.

[8] A. B. Nair *et al.*, "Design, Development, and Evaluation of Constant Voltage Iontophoresis for the Transungual Delivery of Efinaconazole," *Pharmaceutics*, 2023, doi: 10.3390/pharmaceutics15051422.

[9] B. Samir, A. El-Kamel, N. Zahran, and L. Heikal, "Resveratrol-loaded invasome gel: A promising nanoformulation for treatment of skin cancer," *Drug Deliv. Transl. Res.*, 2024, doi: 10.1007/s13346-024-01534-9.

[10] B. C. Y. Lee, M. S. Mahtab, T. H. Neo, I. H. Farooqi, and A. Khursheed, "A comprehensive review of Design of experiment (DOE) for water and wastewater treatment application - Key concepts, methodology and contextualized application," 2022. doi: 10.1016/j.jwpe.2022.102673.

[11] S. Govindarajan and I. V. Asharani, "Development and Validation of a LC-MS/MS Method for the Profiling of Impurities Formed during Stress Study of Antifungal Agent-Efinaconazole," *J. Chromatogr. Sci.*, 2022, doi: 10.1093/chromsci/bmab079.

[12] E. Papadopoulos, B. C. Arrahmani, K. Beck, and W. Friess, "Lyso-phosphatidylcholine as an interfacial stabilizer for parenteral monoclonal antibody formulations," *Eur. J. Pharm. Biopharm.*, 2024, doi: 10.1016/j.ejpb.2024.114514.

[13] F. Orabona *et al.*, "Tuning grafted catalysts for the selective conversion of carbon dioxide into limonene-based cyclic carbonates," *Appl. Catal. B Environ.*, 2026, doi: 10.1016/j.apcatb.2025.126137.

[14] R. A. Vlad *et al.*, "Hydroxypropyl Methylcellulose—A Key Excipient in Pharmaceutical Drug Delivery Systems," 2025. doi: 10.3390/pharmaceutics17060784.

[15] Y. Sun *et al.*, "Toxicity of humectants propylene glycol and vegetable glycerin in electronic nicotine delivery systems," 2025. doi: 10.1016/j.toxlet.2025.111739.

[16] S. R. Lipner, A. K. Gupta, W. S. Joseph, B. Elewski, E. Guenin, and T. C. Vlahovic, "Efficacy and Safety of Efinaconazole 10% Topical Solution for Treatment of Onychomycosis in Older Adults: A Post Hoc Analysis of Two Phase 3 Randomised Trials," *Mycoses*, 2025, doi: 10.1111/myc.70069.

[17] R. M. Almuqbil, N. Sreeharsha, and A. B. Nair, "Formulation-by-Design of Efinaconazole Spanlastic Nanovesicles for Transungual Delivery Using Statistical Risk Management and Multivariate Analytical Techniques," *Pharmaceutics*, 2022, doi: 10.3390/pharmaceutics14071419.

[18] A. K. Gupta, A. Mann, S. Polla Ravi, T. Wang, and E. A. Cooper, "Efinaconazole 10% solution: a comprehensive review of its use in the treatment of onychomycosis," 2024. doi: 10.1080/14656566.2024.2416924.

[19] V. Swathi and G. V. Radha, "DEVELOPMENT AND EVALUATION OF PRONIOSOMAL GEL FOR ENHANCING THE TRANSDERMAL DELIVERY OF EFINACONAZOLE," *Asian J. Pharm. Clin. Res.*, 2025, doi: 10.22159/ajpcr.2025v18i4.53920.

[20] I. B. T. SUNDARI, S. KALVA, and M. BINDU, "DEVELOPMENT OF EFINACONAZOLE NAIL GEL FOR THE TREATMENT OF ONCHOMYCOSIS," *Int. J. Curr. Pharm. Res.*, 2023, doi: 10.22159/ijcpr.2023v15i6.3092.